

# Effect of surface states of layered double hydroxides on conductive and transport properties of nanocomposite polymer electrolytes

Chien-Shiun Liao\*, Wei-Bin Ye

*Department of Chemical Engineering, Yuan-Ze University, 135 Yuan-Tung Road, Taoyuan 320, Taiwan, ROC*

Received 17 March 2004; received in revised form 2 June 2004; accepted 9 June 2004

## Abstract

All solid-state poly(ethylene oxide) (PEO) nanocomposite electrolytes were made containing nanoscale fillers of layered double hydroxides (LDHs). Two kinds of LDHs with different surface states were prepared by aqueous co-precipitation method. The LDHs were added into PEO matrix to study the structures, conductivities and ionic transport properties of nanocomposite electrolytes. The structures of LDHs were characterized by infrared spectra, thermogravimetric analysis and wide-angle X-ray diffraction. With enhanced compatibility of LDH sheets by oligo(ethylene oxide) surface modification, the PEO/OMLDH nanocomposite electrolyte exhibits an amorphous morphology and an enhancement of conductivity by three orders of magnitude as compared to pure PEO electrolyte. The lithium ion transference number  $T_{\text{Li}^+}$  of PEO/LDH nanocomposite electrolyte measured with a value of 0.42 is two times higher than the one of pure PEO electrolyte, which can be attributed to the Lewis acid–base interaction between surface states of metal hydroxides and counter anions of lithium salts. © 2004 Elsevier B.V. All rights reserved.

**Keywords:** Nanocomposite; Electrolytes; LDH

## 1. Introduction

Solid polymer electrolytes composed with poly(ethylene oxide)s (PEOs) exhibit high ionic conductivities, stable electrochemical characteristics and excellent mechanical properties, which lead to play an important role in the development of Li-ion polymer rechargeable batteries [1]. Two important properties viz. ionic conductivity and lithium ion transference number ( $T_{\text{Li}^+}$ ) are of particular concerned for PEO-based polymer electrolytes. The former relates to the power density and the latter one to the current density and cycleability of rechargeable batteries [2]. Due to the retardation of lithium ion transport imposed by the crystalline phase of PEO, higher ionic conductivity of pure PEO electrolyte only can be achieved in the molten or amorphous state. Besides the Li ions transport in the PEO-Li<sup>+</sup> complex, the mobile counter anions and ion-pairs also contribute to the ionic conductivities that would lower the values of  $T_{\text{Li}^+}$  [3]. In this work, the PEO-layered double hydroxide (LDH)-LiClO<sub>4</sub> nanocomposites electrolytes were prepared

to study the effect of different surface states of LDHs on the ionic conductivities and  $T_{\text{Li}^+}$ .

To enhance conductivities at ambient temperature, the PEO nanocomposite electrolytes containing nanoparticles of metal oxides as fillers were reported by Scrosati and co-workers [4]. The ceramic nanoparticles performed as solid plasticizers for PEO to inhibit crystallization on annealing from molten state, which increased the conductivities to around  $10^{-5} \text{ S cm}^{-1}$  at room temperature. Thus, the recent research efforts in PEO-based polymer electrolytes have been directed to the nanocomposite polymer electrolytes by use of miscellaneous nanoparticles such as TiO<sub>2</sub>, Al<sub>2</sub>O<sub>3</sub>, SiO<sub>2</sub>, ZnO and MgO [5–9]. Meanwhile, there are majority of studies for polymer nanocomposites by using layered silicate compounds of montmorillonite (MMT) to disperse or exfoliate into various polymer matrixes [10]. In the previous studies of PEO/MMT nanocomposite polymer electrolytes, the Li<sup>+</sup> intercalated MMT was dispersed into PEO matrix by solution [10] or melt [11] blending. The PEO-Li<sup>+</sup> complex formed on the surface region of layered silicates. Due to the immobility of negative charges bound on the surface of silicates, only Li<sup>+</sup> cation transport could occur. This single-ion transport behavior characterized with an estimated value of  $T_{\text{Li}^+} = 1$ . The negative sites located on the layer surface

\* Corresponding author. Tel.: +886-3-4638800x567;  
fax: +886-3-4559373.

E-mail address: [csliao@saturn.yzu.edu.tw](mailto:csliao@saturn.yzu.edu.tw) (C.-S. Liao).

also trapped the  $\text{Li}^+$  cations to block the transport of conducting cations. A higher conductivity only could be obtained at temperature above 400 K [11]. Alternately, the surfactant modified MMT was used as a nanoscale-dispersing agent to blend with PEO matrix. The PEO-rich phase favored the formation of MMT exfoliated nanocomposite and enhanced the ionic conductivity [12]. As contrast to the negative charges located on the layered silicates of MMT, another class of inorganic layered materials with positive charged surface such as LDH has been reported for the preparation of nanocomposite polymer electrolytes in our previous work [13]. The results show that the PEO nanocomposite electrolytes with oligo(ethylene oxide) modified LDHs exhibit exfoliation morphology and high conductivities at ambient temperature. We further perform the studies of different surface states of LDHs affecting on the conductivities and  $T_{\text{Li}^+}$  values of PEO nanocomposite electrolytes in this work.

## 2. Experimental

The pristine LDH was prepared following a standard aqueous co-precipitation and thermal crystallization method [14]. A mixture of equal molar ratio of mono- and bi-hydroxy PEO phosphonate (PEOPA) was synthesized by poly(ethylene glycol) methyl ether ( $M_n = 550$ ) and  $\text{P}_2\text{O}_5$  in benzene solution according to literature procedures [15]. The PEOPA modified LDHs (OMLDH) were prepared following the template method [16] and the experimental details were described in our previous work [13]. PEO-based nanocomposite polymer electrolytes with 10 wt.% of LDH additives were formed by mixing of PEO ( $M_v = 6 \times 10^5$ ; Aldrich), pristine LDH (or OMLDH) and lithium perchlorate ( $\text{LiClO}_4$ ; Aldrich) in anhydrous acetonitrile operated in a dry box, where PEO and  $\text{LiClO}_4$  were dried previously in a vacuum oven at  $60^\circ\text{C}$  for 3 days and LDH (or OMLDH) dried at  $200^\circ\text{C}$  for 30 min to remove the interlayer water. After continuous stirring at  $70^\circ\text{C}$  for 24 h, the solution mixture was cast on the Teflon sheet maintained at  $40^\circ\text{C}$  for 48 h under  $\text{N}_2$  and a further drying in a vacuum oven at  $60^\circ\text{C}$  for 24 h. The quantity of lithium salt added into the polymer electrolyte was calculated at a molar ratio of  $[\text{ethylene oxide}]/[\text{Li}^+] = 8$  in this work.

X-ray diffraction data between  $2^\circ$  and  $45^\circ$   $2\theta$  were collected at  $1^\circ \text{min}^{-1}$  on a Shimadzu XRD6000 diffractometer equipped with nickel-filtered  $\text{Cu K}\alpha$  radiation operated at 40 kV and 30 mA. Infrared spectra were obtained using a Bruker IFS 28 FTIR spectrometer in the transmission mode from 400 to  $4000 \text{cm}^{-1}$  with a  $2 \text{cm}^{-1}$  resolution. A thermogravimetric analyzer (TA, TGA-2950) was used to measure weight losses of LDH samples under a nitrogen stream from 30 to  $600^\circ\text{C}$  with a heating rate of  $10^\circ\text{C min}^{-1}$ . The fractured surface of the PEO/OMLDH nanocomposite was sputtered with gold and analyzed by field emission SEM (JEOL JSM-6340F). Ionic conductivity was measured using the ac impedance techniques with a Solartron 1255B frequency re-

sponse analyzer in the temperature range  $10\text{--}90^\circ\text{C}$ , where the given nanocomposite electrolyte films were placed sandwiched between two polished stainless-steel blocking electrodes. The lithium ion transference number,  $T_{\text{Li}^+}$ , was evaluated using the technique combined dc and ac electrode polarizations by imposing a voltage pulse to a cell composed with two non-blocking Li-electrodes and one sandwiched polymer electrolyte film [17,18].

## 3. Results and discussion

X-ray diffraction data (XRD) for pristine LDH and OMLDH are shown in Fig. 1. The strong Bragg reflection peak appeared at  $2\theta = 11.4^\circ$  for pristine LDH was attributed to the reflections of (00 $l$ ) series planes diffraction. The interlayer spacing of  $7.7 \text{\AA}$  calculated from Bragg's equation was contributed from the thickness of metal hydroxide sheet ( $\sim 4.8 \text{\AA}$ ) and the gallery region contained intercalated anions ( $\sim 2.9 \text{\AA}$ ) [16]. This XRD pattern exhibits the characteristic reflections of carbonate intercalated LDH [19], which indicates the carbonate being the dominating intercalated anion resulted from the contaminant of environmental  $\text{CO}_2$ . While for OMLDH, there was only a weak broad reflection appeared at  $2\theta = 8.4^\circ$  ( $d$  spacing =  $10.5 \text{\AA}$ ), without any sharp and apparent diffraction peaks caused by carbonate, indicating that there is little long-range order in the  $c$ -direction of LDH crystallites. Subtracting the thickness of metal hydroxide, anionic oligo(ethylene oxide) accommodates the gallery region with a thickness of  $5.7 \text{\AA}$ . This renders the PEO oligomer chains adopting a disordered and liquid-like conformation confined between layered double hydroxides, which are similar with the results of intercalated PEO/MMT nanocomposites system [20].

FTIR spectra for pristine LDH and OMLDH are shown in Fig. 2. Both LDH and OMLDH display the typical features of  $\text{Mg}_2\text{Al}(\text{OH})_6$  layered double hydroxide. A very strong and broad absorption in the region between  $3000$  and  $3700 \text{cm}^{-1}$  was attributed to the stretching mode of hydroxyl group ( $\nu_{\text{OH}}$ ) due to the hydrogen bonding of  $-\text{OH}$  group in the layered structures [21]. The characteristic

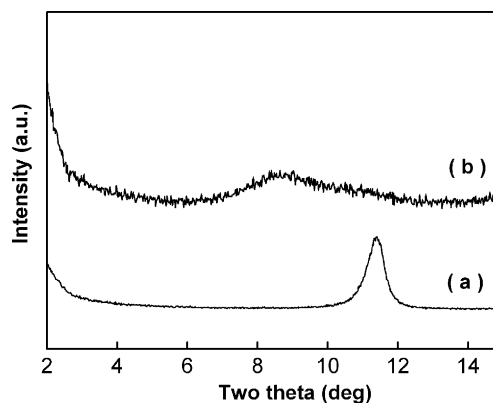


Fig. 1. X-ray diffraction patterns of (a) LDH and (b) OMLDH.

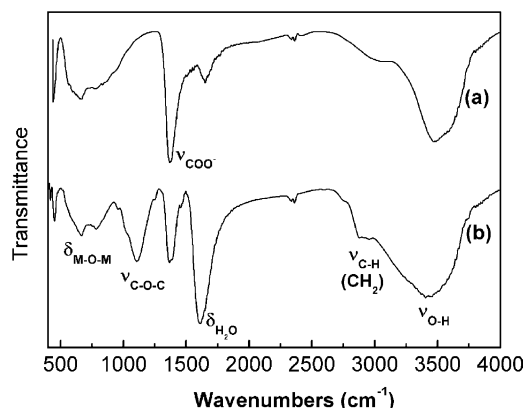


Fig. 2. FTIR spectra of (a) LDH and (b) OMLDH.

absorption peaks for MO vibrations and MOH bending appeared at 785, 665 and 450  $\text{cm}^{-1}$  [19], where M represented the metal cations of  $\text{Mg}^{2+}$  or  $\text{Al}^{3+}$  in the metal hydroxides. Besides the absorption bands of metal hydroxides, a sharp absorption band at 1360  $\text{cm}^{-1}$  can be assigned as the carbonate stretching mode ( $\nu_3$ ) resulted from the interlayer containment  $\text{CO}_3^{2-}$  [22]. The absorption band at 1610  $\text{cm}^{-1}$  was attributed to the bending mode of interlayer water  $\delta_{\text{H}_2\text{O}}$ . The characteristic  $\text{CH}_2$  symmetrical stretching mode at 2858  $\text{cm}^{-1}$  and  $\text{CH}_2$  asymmetrical stretching mode at 2927  $\text{cm}^{-1}$  were observed in the spectrum of OMLDH resulted from the intercalated oligo(ethylene oxide) surfactant [23]. The new aliphatic  $\nu(\text{C}-\text{O}-\text{C})$  absorption bands of the oligo(ethylene oxide) at 1244 and 1039  $\text{cm}^{-1}$  were distinguished in the spectrum of OMLDH, which indicated the effective intercalation of PEO phosphonate (PEOPA) into the LDHs.

Thermal behavior of the prepared LDH samples was analyzed by TGA as shown in Fig. 3. For pristine LDH, the characterized transition at low temperature (below 210  $^{\circ}\text{C}$ ) corresponds to the evaporation of absorbed water in surface and interlayer of LDHs with a weight loss of 11 wt.%. The second transition begins at about 270  $^{\circ}\text{C}$  and ends at 360  $^{\circ}\text{C}$ , which is attributed to the decomposition of intercalated car-

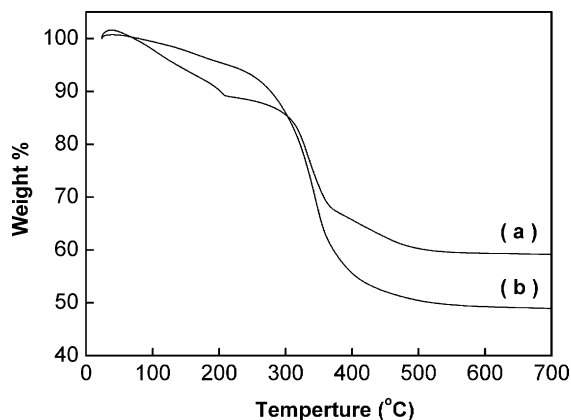


Fig. 3. TGA thermogram of (a) LDH and (b) OMLDH.

bonate. The third transition begins at about 360  $^{\circ}\text{C}$  and ends at 470  $^{\circ}\text{C}$  results from the dehydroxylation of the metal hydroxide. On the other hand, the weight loss for OMLDH is characterized with two transition temperatures. The first transition below 260  $^{\circ}\text{C}$  is attributed to the weight loss of absorbed water. The second one begins at about 270  $^{\circ}\text{C}$  and ends at 470  $^{\circ}\text{C}$ , which is attributed to the decomposition of intercalated oligo(ethylene oxide) along with dehydroxylation of metal hydroxides. The total weight loss for OMLDH (50.0 wt.%) is larger than the one of pristine LDH (40.0 wt.%) that can be attributed to the intercalation of PEO oligomer.

To prepare the nanocomposite polymer electrolytes, the pre-dried lithium salt  $\text{LiClO}_4$  was added into the pure PEO and PEO/LDH nanocomposites at a molar ratio of  $[\text{ethylene oxide}]/[\text{Li}^+] = 8$  under anhydrous condition. The XRD pattern of pure  $(\text{PEO})_8\text{-LiClO}_4$  polymer electrolyte (Fig. 4a) exhibits diffraction peaks at  $2\theta = 15.2^{\circ}$ ,  $22.6^{\circ}$  and  $23.8^{\circ}$ , which are attributed to the formation of coexisted crystalline complex phase of  $\text{PEO}_6\text{:LiClO}_4$  [24,25]. As the lithium salt was added into PEO/LDH nanocomposite, the characteristic diffraction peaks of crystalline  $\text{PEO-Li}^+$  complex disappeared. Instead, an amorphous halo around  $2\theta = 16\text{--}28^{\circ}$  and a weak diffraction peak at  $10^{\circ}$  appeared as shown in Fig. 4b. The former is due to the PEO amorphous phase with dissolved salt and the latter is attributed to the agglomerate LDH sheets. It indicates that the PEO chain is partially intercalated between the metal hydroxide layers with a parallel stacking structure. The PEO/LDH nanocomposite can be assigned as an intercalated type nanocomposite. On the other hand, the PEOPA with mono- or bi-hydroxy oligo(ethylene oxide) connected in phosphonate behaves as a lipid structure with long chains. As the PEOPA ionic bonding to OMLDH by in situ template synthesis, the hydrophilic PEO chain segments can interact strongly with metal hydroxide. The high-density location of PEOPA between LDH sheets results into a distorted conformation due to the steric hindrance of

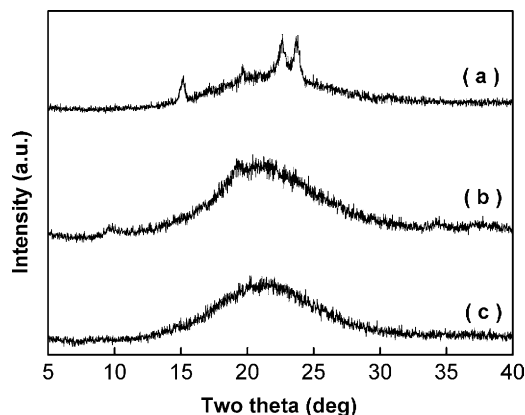


Fig. 4. X-ray diffraction patterns of (a) pure PEO, (b) PEO/LDH nanocomposites, and (c) PEO/OMLDH nanocomposites with 10 wt.% of filler loading and the quantity of lithium salt added into the polymer electrolytes at a molar ratio of  $[\text{ethylene oxide}]/[\text{Li}^+] = 8$ .

long flexible PEO chains in OMLDH. Usually, the liquid plasticizer is added into the crystalline polymer to suppress the growth of crystalline domain. The compatible interaction between plasticizer and polymer matrix will disrupt the ordered structure packing of polymer segments. Where the plenty dispersion of PEOPA modified metal hydroxide sheets in PEO/OMLDH nanocomposite can play a role of nanoscale solid plasticizer to inhibit the crystal growth of PEO. There are no apparent XRD peaks at  $2\theta = 2\text{--}10^\circ$  for PEO/OMLDH nanocomposite as shown in Fig. 4c. It indicates that the  $d$ -spacing of intercalated layers is larger than  $44\text{ \AA}$ . An exfoliated type of nanocomposite with disrupted layer registry is purposed for the PEO/OMLDH nanocomposites. Under such condition, the added lithium cations can only complex with ethylene oxide segments in the PEO-rich domain and form an amorphous phase. Though the direct image evidence for OMLDH exfoliation by transmission electron micrograph is absent, the indirect evidence of much reduced domain size due to the addition of exfoliated OMLDH layers is discussed as followed. The higher magnification ( $100,000\times$ ) of secondary electron image for PEO/OMLDH nanocomposite shows that the average domain size is about  $25\text{ nm}$  as shown in Fig. 5. In comparison, the average size of the crystalline domain appeared in the pure PEO is about  $50\text{ }\mu\text{m}$ , meaning that the crystal growth of PEO proceeds without disturbance. The smaller domain size existed in the PEO/OMLDH nanocomposite can be attributed to the confinement effect of LDH particle size by PEOPA during the LDH crystallization. It is consistent with the results of polystyrene sulfonate (PSS)/LDH system, where the LDH particle size is about  $20\text{--}25\text{ nm}$  resulted from the nucleation promotion by PSS [16].

Fig. 6 shows the temperature dependence of ionic conductivities of pure polymer electrolyte (PEO)<sub>8</sub>-LiClO<sub>4</sub> and the nanocomposite electrolytes with lithium salt addi-

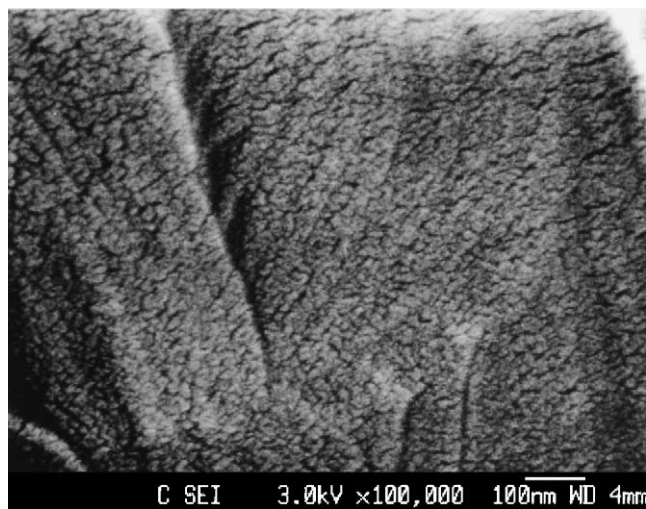


Fig. 5. SEM secondary electron images of PEO/OMLDH nanocomposite with 10 wt.% of filler loading and the quantity of lithium salt added into the polymer electrolyte at a molar ratio of [ethylene oxide]/[Li<sup>+</sup>] = 8.

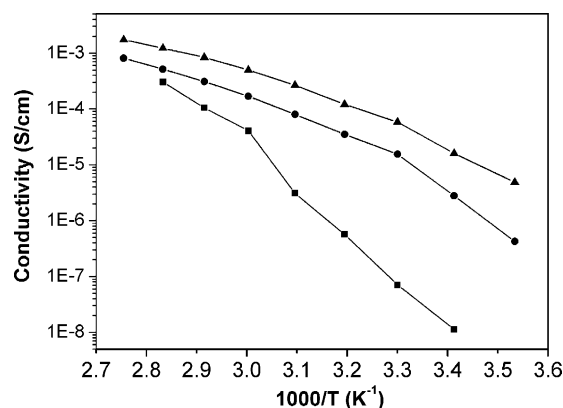


Fig. 6. Arrhenius plots of the ionic conductivity of pure PEO (■), PEO/LDH nanocomposites (●), and PEO/OMLDH nanocomposites (▲) with 10 wt.% of filler loading and the quantity of lithium salt added into the polymer electrolytes at a molar ratio of [ethylene oxide]/[Li<sup>+</sup>] = 8.

tion. At ambient temperature ( $20^\circ\text{C}$ ), the conductivities of nanocomposite electrolytes PEO/OMLDH and PEO/LDH are  $1.61 \times 10^{-5}$  and  $2.79 \times 10^{-6}\text{ S cm}^{-1}$ , which are higher than  $1.14 \times 10^{-8}\text{ S cm}^{-1}$  of PEO by three and two orders of magnitude, respectively. In addition, the typical Vogel–Tamman–Fulcher (VTF) type curvature of the  $\log \sigma$  versus  $1/T$  plots for nanocomposite electrolytes system within the whole temperature range indicate the characteristics of completely amorphous polymer electrolyte system. However, the temperature dependence of conductivity for pure PEO polymer electrolyte shows a distinct transition around the melting temperature ( $60^\circ\text{C}$ ) of PEO due to the crystalline–amorphous transition. The observed enhancement and VTF-type dependence of ionic conductivities for nanocomposite electrolyte system as compared to the pure PEO polymer electrolyte are consistent with the results of XRD. This behavior is attributed to the formation of PEO-rich amorphous phase resulted from the solid plasticizer effect of exfoliated compatible OMLDH layers or intercalated LDH agglomerates. The higher conductivity of PEO/OMLDH than PEO/LDH can be explained as a higher degree dispersion of compatible OMLDH layers in the PEO matrix. To elucidate the different surface states of metal hydroxides on the Li<sup>+</sup> ion transport, the  $T_{\text{Li}^+}$  measurement was performed and discussed as followed.

To determine the lithium ion transference number,  $T_{\text{Li}^+}$ , a non-blocking cell of Li/electrolyte/Li configuration was composed. A dc potential difference  $\Delta V$  was applied across the electrolyte, the initial current  $I_0$  and the steady-state current  $I_s$  were determined from the time evolution of the resulting current flow as shown in Fig. 7. On the meantime, the initial and steady-state interfacial resistance as  $R_0$  and  $R_s$  were measured along with the impedance Nyquist plots taken before and after the pulse application to correct the change in impedance of the test cell during polarization as shown in Fig. 8. The values of lithium ion transference



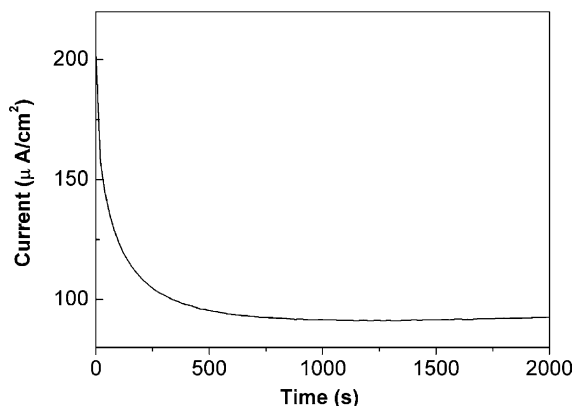


Fig. 7. Current–time curve of a PEO/LDH nanocomposites with 10 wt.% of filler loading and the quantity of lithium salt added into the polymer electrolytes at a molar ratio of [ethylene oxide]/[Li<sup>+</sup>] = 8.

number  $T_{Li^+}$  can be described as follows [17,18]:

$$T_{Li^+} = \frac{I_s(\Delta V - I_0 R_0)}{I_0(\Delta V - I_s R_s)} \quad (1)$$

The  $T_{Li^+}$  values measured at 90 °C are 0.21, 0.42, and 0.30 for pure PEO, PEO/LDH, and PEO/MOLDH nanocomposites, respectively. Due to the characteristics of a positive electrophoretic mobility and the Lewis acid –OH groups located on the surface of metal hydroxide for pristine LDH [16], a strong Lewis acid–base interaction between the LDH surface states and the counter anions  $ClO_4^-$  will occur. A preferred  $Li^+$  transport is promoted resulted from the dissociation of  $LiClO_4$  salt and the pinning effect of counter anions at the surface of LDH sheets. Thus, the  $T_{Li^+}$  value is enhanced from 0.21 of pure PEO electrolyte to 0.42 of PEO/LDH nanocomposite electrolyte. However, the surface modification by compatible oligomeric PEO moieties of PEO/OMLDH system provides a steric hindrance for the direct interactions of anions and surface groups of LDH layers that cause only a little enhancement of  $T_{Li^+}$ . These observations are consistent with the transport model for the composite polymer electrolytes [26], where the ionic transport

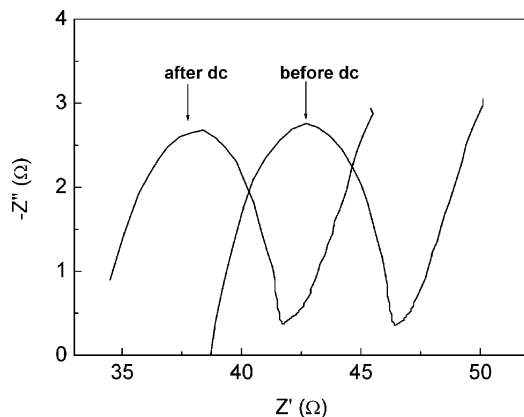


Fig. 8. Nyquist plots of a PEO/LDH nanocomposites with 10 wt.% of filler loading and the quantity of lithium salt added into the polymer electrolytes at a molar ratio of [ethylene oxide]/[Li<sup>+</sup>] = 8.

through Lewis acid–base interactions between the surface states and the ionic species dominate the enhancement of  $T_{Li^+}$ .

#### 4. Conclusions

The organic modification of layered double hydroxide (OMLDH) is synthesized with PEO phosphonate by the template method. The OMLDH is dispersed into the PEO matrix by solution mixing to form an exfoliated PEO/OMLDH nanocomposite. The nanoscale dispersion of metal hydroxide layers acts as solid plasticizers resulting in formation of stable amorphous phase in nanocomposite. A conductivity of  $1.61 \times 10^{-5} \text{ S cm}^{-1}$  for PEO/OMLDH nanocomposite electrolyte is higher than the pure PEO electrolyte by three orders of magnitude at ambient temperature. On the other hand, the Lewis acid characteristics appeared on the surface group of pristine LDH causes an effective lithium salt dissociation and pinning effect of counter anions. The  $T_{Li^+}$  of PEO/LDH nanocomposite electrolyte measured with a value of 0.42 is two times higher than the one of pure PEO electrolytes, which can be attributed to the Lewis acid–base interactions between surface states of LDH and anionic species. Hence, the results observed here provide a further optimization strategy to apply the novel PEO/LDH nanocomposite polymer electrolytes with high conductivities and  $T_{Li^+}$  values in the rechargeable lithium ion-polymer batteries.

#### Acknowledgements

We thank the National Science Council of ROC for financial aid through Project NSC 90-2216-E-155-002.

#### References

- [1] F.B. Dias, L. Plomp, J.B.J. Veldhus, J. Power Sour. 88 (2000) 169.
- [2] F.M. Gray, Polymer Electrolytes, Royal Soc. Chem., Materials Monograph, 1997.
- [3] F. Croce, G.B. Appetecchi, L. Persi, B. Scrosati, Nature 394 (1998) 456.
- [4] F. Croce, R. Curini, A. Martinelli, L. Persi, F. Ronci, B. Scrosati, R. Caminiti, J. Phys. Chem. B 103 (1999) 10632.
- [5] C. Capiglia, P. Mustarelli, E. Quartarone, C. Tomasi, A. Magistris, Solid State Ionics 118 (1999) 73.
- [6] H.-M. Xiong, X. Zhao, J.-S. Chen, J. Phys. Chem. B 105 (2001) 10169.
- [7] B. Kumar, L. Scanlon, R. Marsh, R. Mason, R. Higgins, R. Baldwin, Electrochim. Acta 46 (2001) 1515.
- [8] F. Croce, L. Persi, B. Scrosati, F. Serraino-Fiory, E. Plichta, M.A. Hendrickson, Electrochim. Acta 46 (2001) 2457.
- [9] M. Alexandre, P. Dubois, Mater. Sci. Eng. R 28 (2000) 1.
- [10] E. Ruiz-Hitzky, P. Aranda, Adv. Mater. 2 (1990) 545.
- [11] R.A. Vaia, S. Vasudevan, W. Krawiec, L.G. Scanlon, E.P. Giannelis, Adv. Mater. 7 (1995) 154.
- [12] H.-W. Chen, C.-H. Chiu, F.-C. Chang, J. Polym. Sci., Part B: Polym. Phys. 40 (2002) 1342.
- [13] C.-S. Liao, W.-B. Ye, J. Polym. Res. 10 (2003) 241.

- [14] W.T. Riechle, *J. Catal.* 94 (1985) 547.
- [15] Y.H. Geng, Z.C. Sun, J. Li, X.B. Jing, X.H. Wang, F.S. Wang, *Polymer* 40 (1999) 5723.
- [16] O.C. Wilson Jr., T. Olorunloyemi, A. Jaworski, L. Borun, D. Young, A. Siriwat, E. Dickens, C. Oriakji, M. Lerner, *Appl. Clay Sci.* 15 (1999) 265.
- [17] J. Evans, C.A. Vincent, P.G. Bruce, *Polymer* 28 (1987) 2324.
- [18] P.G. Bruce, C.A. Vincent, *J. Electroanal. Chem.* 225 (1987) 1.
- [19] V. Rives, M.A. Ulibarri, *Coord. Chem. Rev.* 181 (1999) 61.
- [20] J. Bujdák, E. Hackett, E.P. Giannelis, *Chem. Mater.* 12 (2000) 2168.
- [21] M. del Acro, C. Martin, I. Martin, V. Rives, R. Trulliano, *Spectrochim. Acta* 49A (1993) 1575.
- [22] C.O. Oriakhi, I.V. Farr, M. Lerner, *J. Mater. Chem.* 6 (1996) 103.
- [23] Z.P. Xu, P.S. Braterman, *J. Mater. Chem.* 13 (2003) 268.
- [24] C.D. Robitaille, D. Fauteux, *J. Electrochem. Soc.* 133 (1986) 315.
- [25] G.S. MacGlasham, Y.G. Andrew, P.G. Bruce, *Nature* 398 (1999) 792.
- [26] J. Przyluski, M. Siekierski, W. Wieczorek, *Electrochim. Acta* 40 (1995) 2251.